Supporting Information

Erat et al. 10.1073/pnas.0812516106

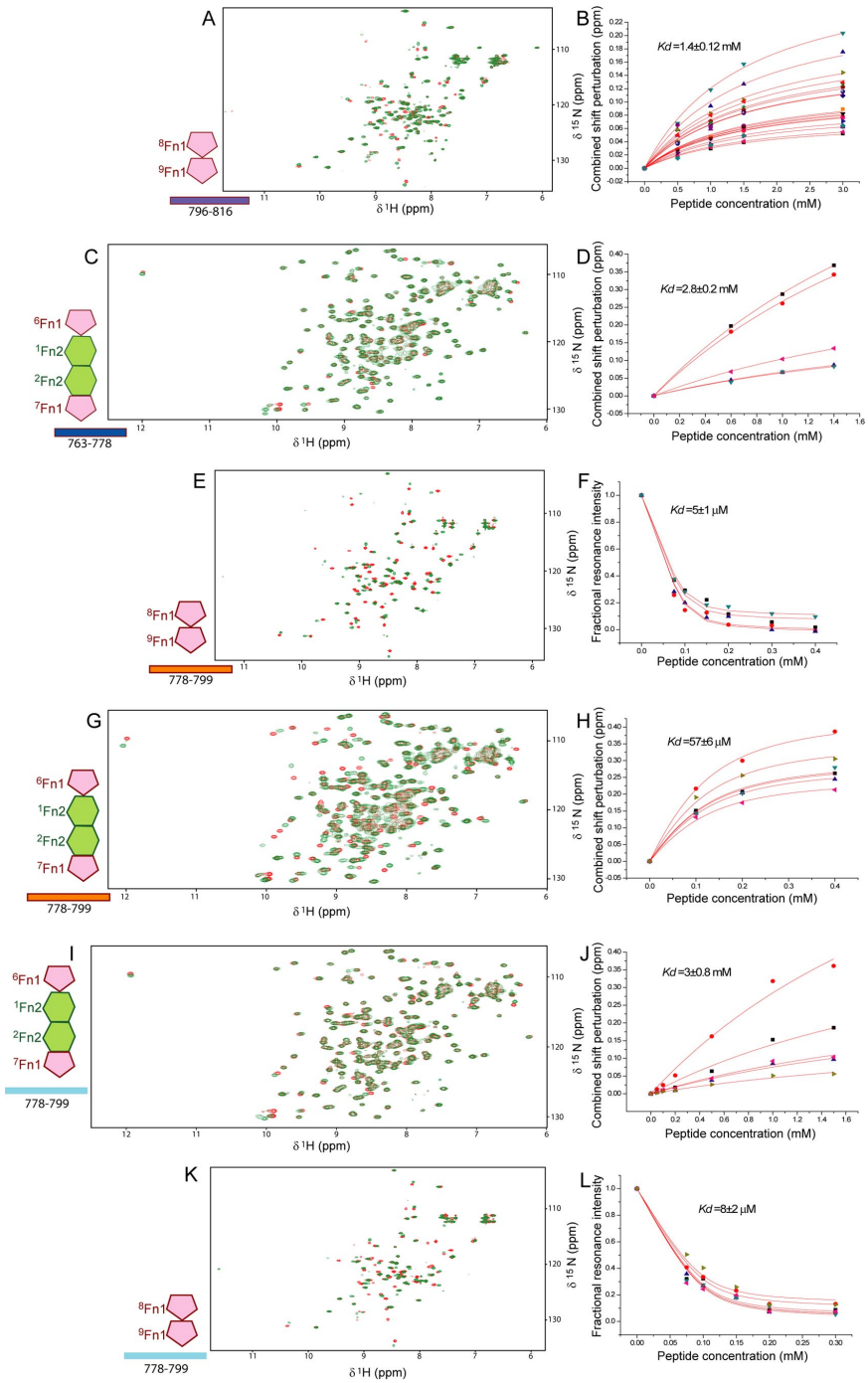

Fig. S1. NMR titrations of collagen peptides to fibronectin fragments. (*A*, *C*, *E*, *G*, *I*, and *K*) ^{15}N-HSQC spectra of the indicated fibronectin fragment at 0.1 mM concentration in PBS, 25 °C ($^{8-9}$FnI) or 20 mM NaPi (pH 7.2), 37 °C (^{6}FnI$^{1-2}$FnII^{7}FnI). Free-protein spectra are shown in red, and spectra in excess of collagen peptide are shown in green. The different peptides used are shown as colored bars (see Fig. 1 in the main manuscript) and the α_1(I) (*A*–*H*) or α_2(I) (*I*–*L*) residue span is provided. (*B*, *D*, *H*, *F*, *L*, and *J*) Plots of combined ^{1}H and ^{15}N chemical shift perturbations (*B*, *D*, *H*, *J*) or free resonance intensities (*F* and *L*) versus peptide concentration for the different NMR titrations. These data were fit to extract equilibrium dissociation parameters assuming a single binding event. The fits are shown as red lines.

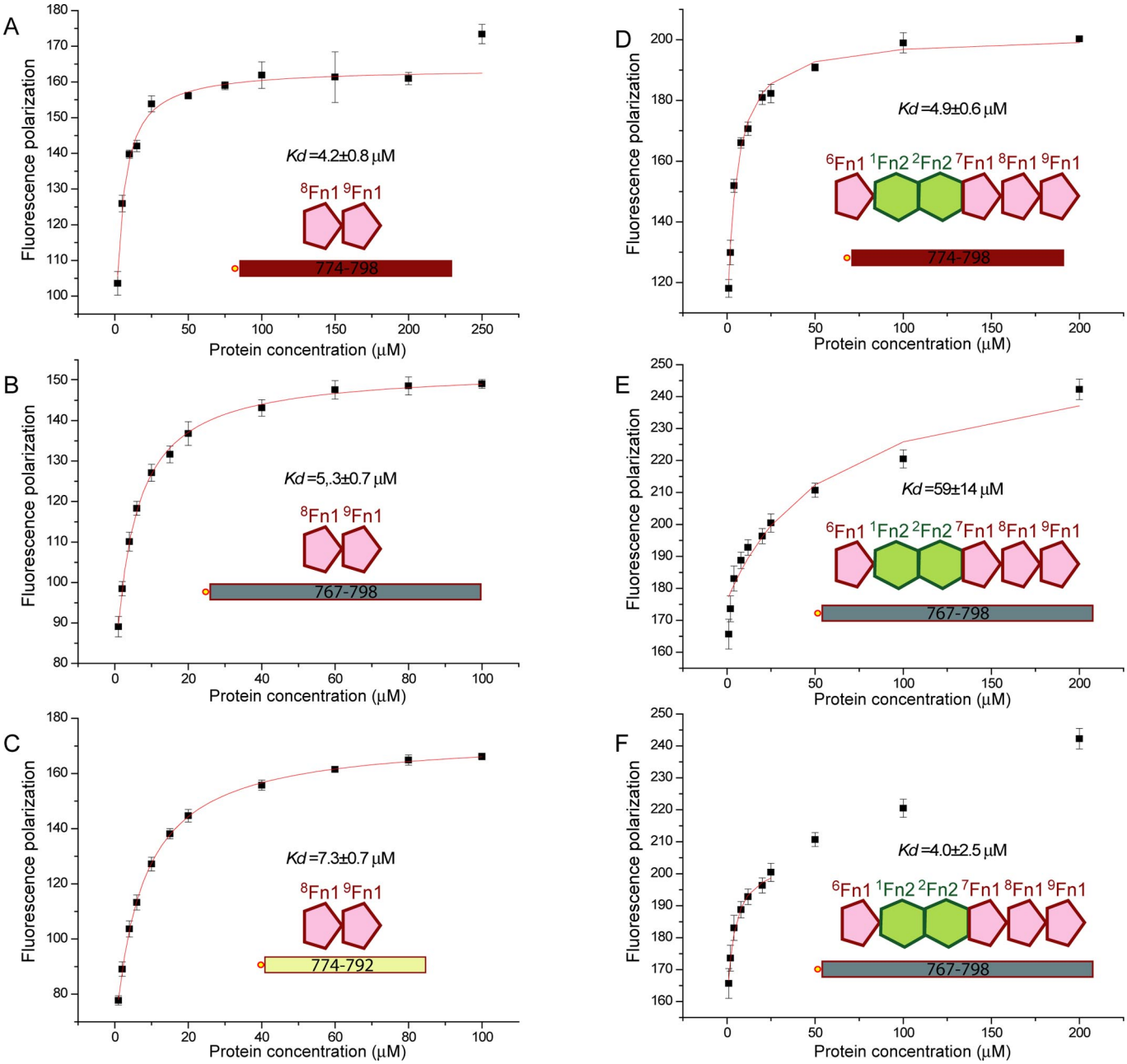

Fig. S2. Fluorescent anisotropy titrations of α_1(I) collagen peptides and fibronectin fragments. Shown here is fluorescent polarization of 75 nM 5-carboxy-fluorescein-labeled peptides [colored bars and α_1(I) residue span] in 150 mM NaCl, 20 mM Tris-Cl buffer (pH 7.4) (TBS), 25 °C versus concentration of the indicated fibronectin fragments. Error bars correspond to 1 standard deviation from 5 sequential anisotropy readouts. Data were fit assuming a single binding event to extract equilibrium parameters. (*A*, *D*) $^{8-9}$FnI and GBD display the same affinity towards a$_1$(I)peptide 774–798, indicating lack of cooperative peptide binding by the GBD sub-fragments. α_1(I) peptide 767–798 (B, *E* and *F*) is N-terminally elongated compared with *D*, and displays evidence of two binding events with GBD. Fitting of the initial 7 points in that titration (*F*) yields a K_d value for the first binding event comparable to that of GBD with α_1(I) peptide 774–798 (*D*). Titration of peptide 767–798 with $^{8-9}$FnI (*B*) does not produce a similar pattern; thus, this effect may be caused by weaker ^{6}FnI$^{1-2}$FnII^{7}FnI interactions to the N-terminal extension. (*C*) Titrations with a C-terminaly truncated peptide and $^{8-9}$FnI show little effect on affinity.

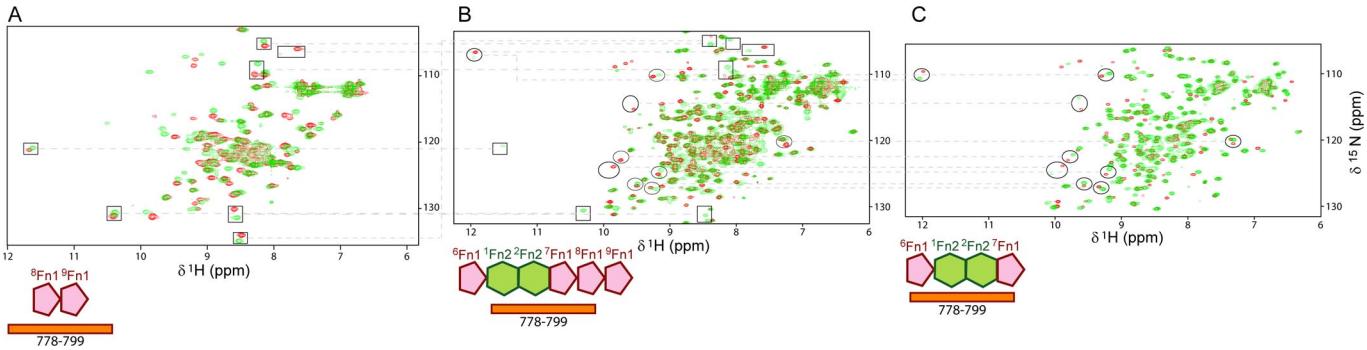

Fig. S3. Binding of α_1(I) collagen peptide to GBD. Shown here are ^{15}N-HSQC spectra of $^{8-9}$FnI (*A*), GBD (*B*), and ^{6}FnI$^{1-2}$FnII^{7}FnI (*C*) in the absence (red) or the presence (green) of a 3-fold excess α_1(I) peptide 778–799. The $^{8-9}$FnI and ^{6}FnI$^{1-2}$FnII^{7}FnI spectra correspond to those in Fig. S1. GBD spectra were acquired in PBS at 37 °C with a 2× excess of peptide for the bound state. GBD resonances perturbed upon binding can be correlated to similar resonances in $^{8-9}$FnI and ^{6}FnI$^{1-2}$FnII^{7}FnI as shown. Because of differences in the ^{15}N sweep width, 2 resonances are differently aliased between the spectra and are connected by vertical lines. A number of $^{8-9}$FnI resonances are absent in the free GBD, likely because of chemical exchange, but appear at frequencies corresponding to the bound state in the presence of peptide.

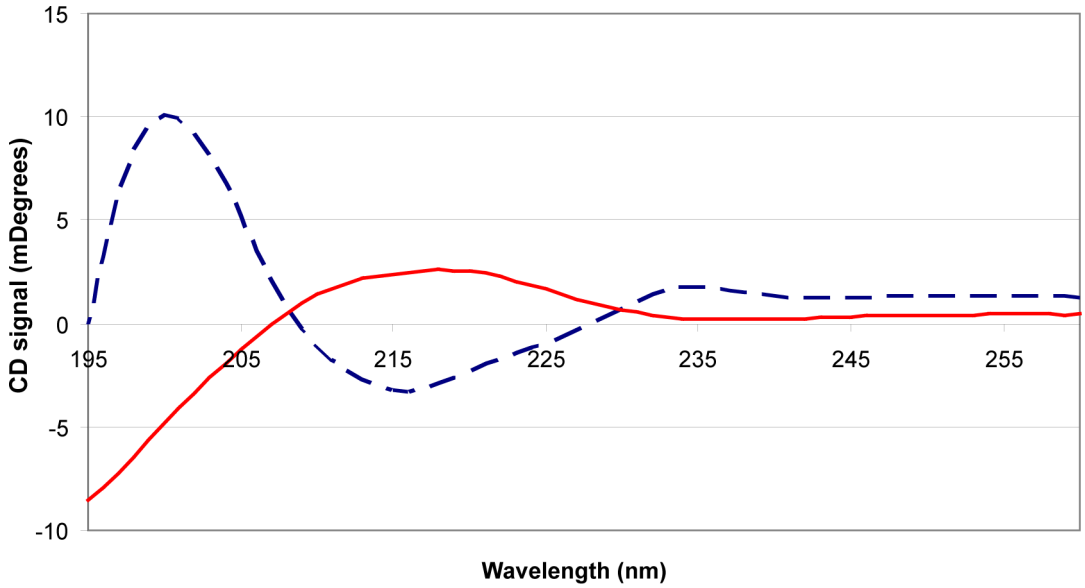

Fig. S4. Circular dichroism spectrum of isolated α_1(I) G_{778}–G_{799} peptide. Shown here are far-UV circular dichroism spectra from a 50 μM sample of α_1(I) G_{778}–G_{799} (solid red line) and a 20 μM sample of the all β-strand FN ^{2}FnIII domain (dashed blue line) (1) in a 150 mM NaCl, 20 mM Na_2HPO_4 (pH 7.2) buffer. The peptide spectrum is substantially different from that of the all-β protein used as reference, having a positive maximum at 218 nm. Such maxima are typically associated with random coil compounds (2), however they are also consistent with polyproline II conformations depending on the amino acid sequence (3).

1. Vakonakis I, Staunton D, Rooney LM, Campbell ID (2007) Interdomain association in fibronectin: Insight into cryptic sites and fibrillogenesis. *EMBO J* 26:2575–2583.
2. Greenfield N, Fasman GD (1969) Computed circular dichroism spectra for the evaluation of protein conformation. *Biochemistry* 8:4108–4116.
3. Darnell G, Orgel JP, Pahl R, Meredith SC (2007) Flanking polyproline sequences inhibit beta-sheet structure in polyglutamine segments by inducing PPII-like helix structure. *J Mol Biol* 374:688–704.

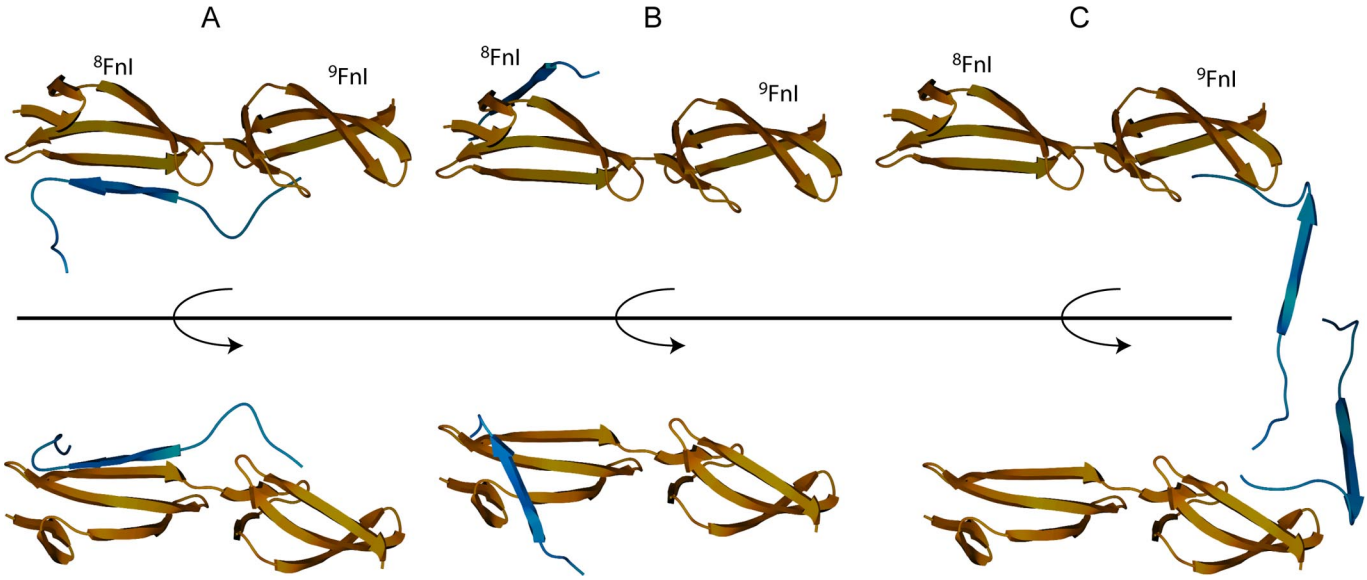

Fig. S5. The different protein–peptide interfaces present in the $^{8-9}$FnI/α_1(I) peptide crystal. The protein is shown in gold and the peptide in blue in 2 orientations. (*A*) The main antiparallel β-strand addition interface described (total area 725 Å^2). (*B*) The peptide β-strand contacts $^{8-9}$FnI strand C in perpendicular orientation, whereas the peptide C terminus contacts the $^{8-9}$FnI B/C loop and strand D (total area 430 Å^2, 30% due to peptide C terminus). (*C*) The peptide C terminus contacts ^{9}FnI strand E in antiparallel orientation (total area 435 Å^2, 80% due to peptide C terminus).

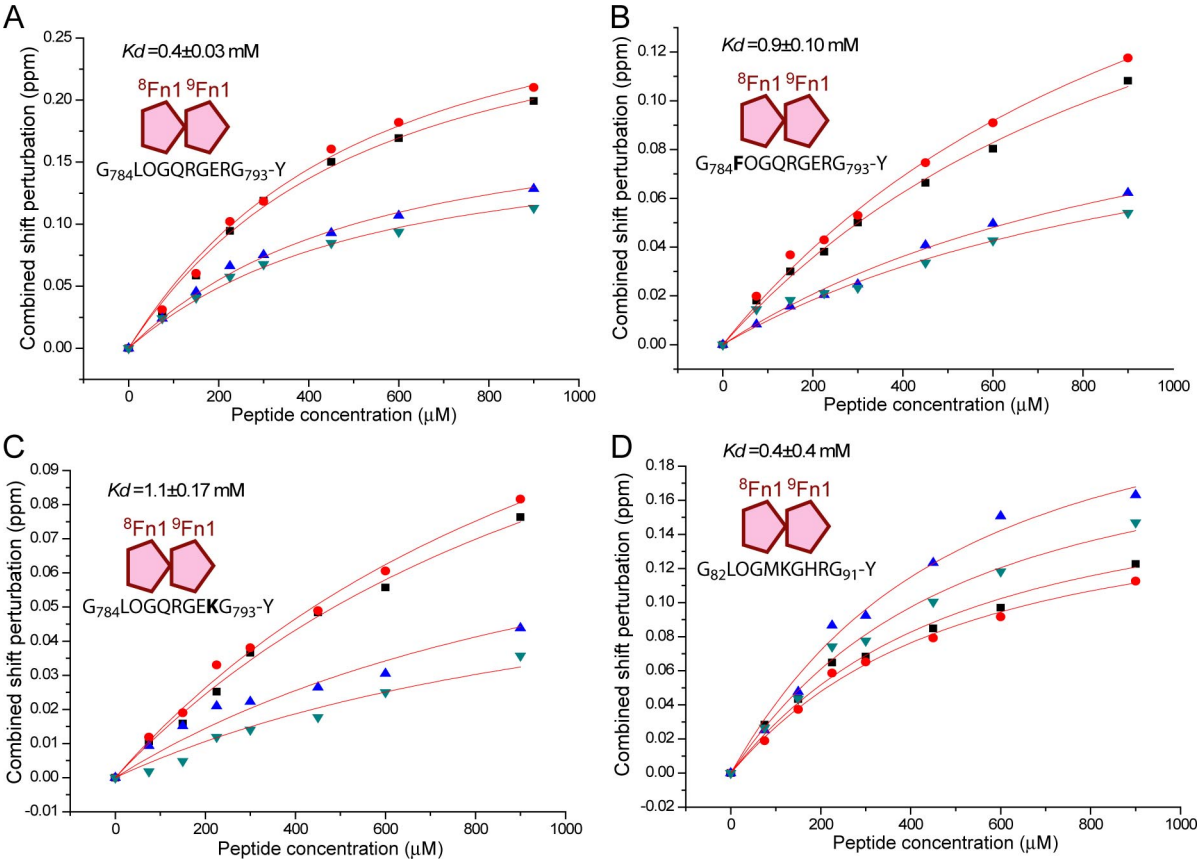

Fig. S6. NMR titrations of short α_1(I) peptides. Shown are plots of combined ^{1}H and ^{15}N chemical shift perturbations versus peptide concentration for NMR titrations of the wild-type core sequence (*A*), sequences bearing single amino acid substitutions (*B* and *C*), or a putative FN-binding sequence identified from analysis of the structure (*D*). Samples were 150 μM ^{15}N $^{8-9}$FnI in PBS buffer at 37 °C and indicated peptide concentration. Even conservative substitutions, shown in bold, on positions 2 (*B*) or 9 (*C*) cause significant changes in the observed affinities.

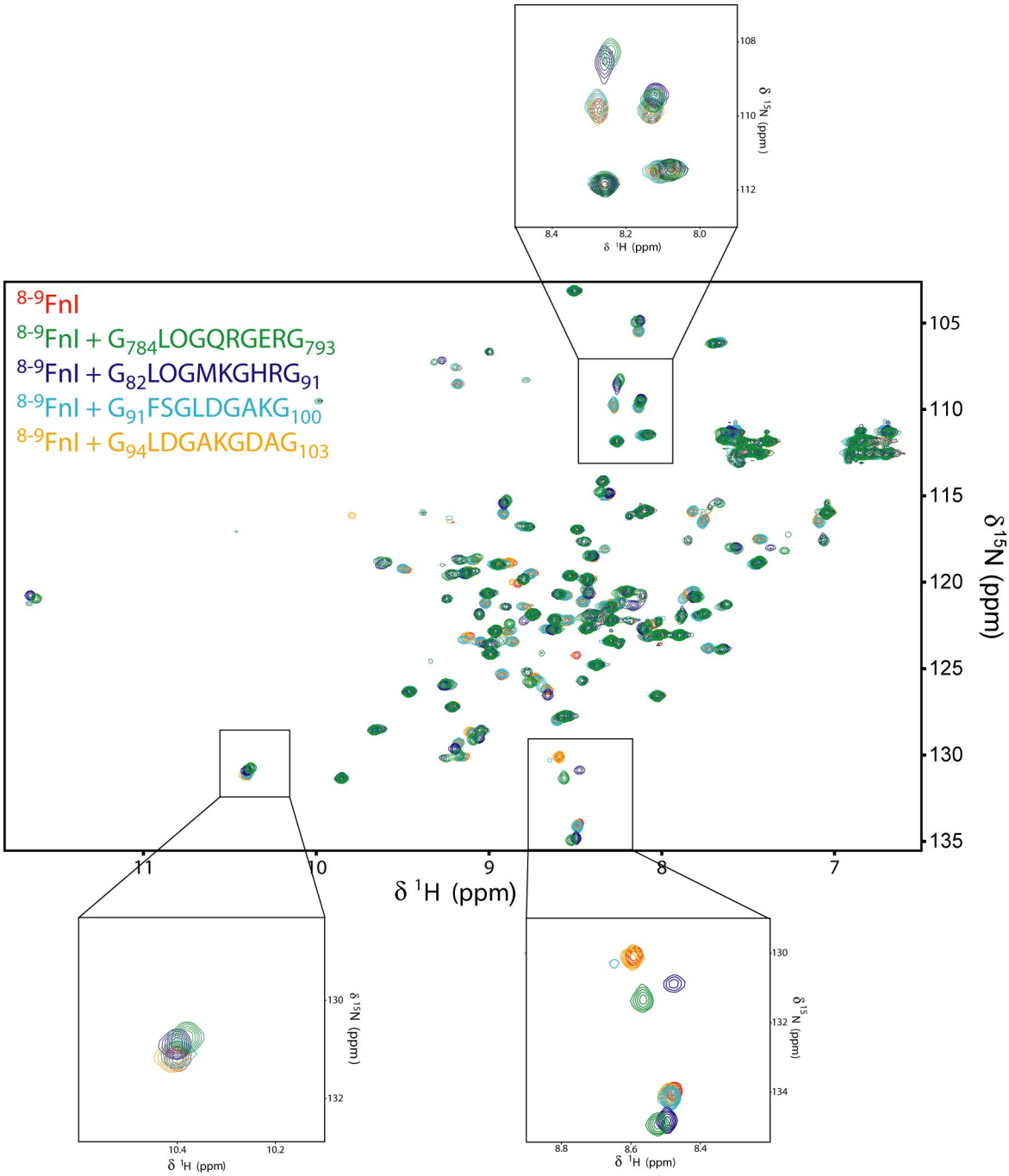

Fig. S7. NMR titrations of alternative α_1(I)-binding sites. ^{15}N-HSQC spectra of $^{8-9}$FnI at 0.15 mM concentration in PBS, 25 °C (red) overlaid with spectra in complex with 0.6 mM peptide. Peptides used correspond to either the core binding sequence derived from the collagenase site of α_1(I), GLPGQRGERG(Y), or putative binding sites identified from the amino acid sequence. As seen, the degree of resonance perturbations varies indicating different binding affinities over these peptides.

Table S1. K_ds of α_1(I) peptides and Fn fragments

Sequence	$^{8-9}$FnI	^{6}FnI$^{1-2}$FnII^{7}FnI	GBD, μM
α_1(I) peptide sequence			ND
GLGGNFAPQLSYGYDEKSTGGISVPGPM-Y	–[†]	–[§]	ND
G_{763}PAGAOGTOGPQGIAG$_{778}$-Y	–[†]	2.8 ± 0.2 mM[§]	ND
G_{778}QRGVVGLOGQRGERGFOGLOG$_{799}$-Y	5 ± 1 μM[†]	57 ± 6 μM	ND
G_{796}LOGPSGEOGKQGPSGASGER$_{816}$-Y	1.4 ± 0.12 mM[†]	–[§,¶]	ND
G_{784}LOGQRGERG$_{793}$-Y	0.4 ± 0.03 mM[‡]	ND	ND
G_{784}FOGQRGERG$_{793}$-Y	0.9 ± 0.10 mM[‡]	ND	ND
G_{784}LOGQRGEKG$_{793}$-Y	1.1 ± 0.17 mM[‡]	ND	ND
G_{784}FOGQRGEKG$_{793}$-Y	–[‡¶]	ND	ND
G_{82}LOGM**K**GHRG$_{91}$-Y	0.4 ± 0.40 mM[‡]	ND	ND
G_{91}**F**SGLDGA**K**G$_{100}$-Y	–[‡¶]	ND	ND
G_{94}LDGAKGDAG$_{103}$-Y	–[‡¶]	ND	ND
*-Q_{774}GIAGQRGVVGLOGQRGERGFOGLO$_{798}$	4.2 ± 0.8 μM	ND	4.9 ± 0.6
*-A_{767} OGTOGPQGIAGQRGVVGLOGQRGERGFOGLO$_{798}$	5.3 ± 0.7 μM	ND	4.0 ± 2.5 [‖]
*-Q_{774}GIAGQRGVVGLOGQRGER$_{792}$	7.3 ± 0.7 μM	ND	ND
α_2(I) peptide sequence			
G_{788}AOGILGLOGSRGERGLOGVAG$_{799}$-Y	8 ± 2 μM[†]	3 ± 0.8 mM[§]	ND

* denotes N-terminal 5-carboxyfluorescein-labeled peptides, affinities for which were determined by fluorescence polarization in 150 mM NaCl, 20 mM Tris-Cl buffer (pH 7.4) (TBS) at 25 °C. Residues involved in amino acid substitutions compared with the wild-type G_{784}–G_{793} sequence are shown in bold type. ND, not determined.

[†]Affinities for unlabeled peptides were determined by NMR in PBS buffer at 25 °C.

[‡]Affinities for unlabeled peptides were determined by NMR in PBS buffer at 37 °C.

[§]Affinities for unlabeled peptides were determined by NMR in 20 mM sodium phosphate (pH 7.2) at 37 °C.

[¶]Very small resonance perturbations were observed; however, they are insufficient to accurately determine affinity.

[‖]Two binding events are evident for α_1(I) peptide 767–798 and GBD; shown is the value of the strongest binding.

Table S2. Crystallographic dataset statistics and model refinement

Data collection	
Cell parameters	$a = b = 56.84$ Å, $c = 150.22$ Å $\alpha = \beta = 90°$, $\gamma = 120°$
Wavelength, Å	0.9796
Resolution, Å	50.06–2.00 (2.10–2.00)
Unique reflections	19,940
R_{merge}	0.065 (0.571)
Completeness, %	100.0 (100.0)
Multiplicity	6.9 (7.1)
$I/\sigma(I)$	18.1 (3.1)
Refinement statistics	
Resolution, Å	49.23–2.10
Unique reflections	17126
Working set	15,897 (92.8%)
Free set	1,229 (7.2%)
R_{work}	0.2090
R_{free}	0.2424
Overall mean B values, Å^2	52.4
No. of amino acid residues per asymmetric unit (protein and ligand)	224
No of water molecules	105
Matthews coefficient	2.63 (water content, 53.34%)
RMSD from ideal values	
Bonds, Å/angles, °	0.008/1.297
Estimated overall coordinate error based on maximum likelihood, Å	0.33
Estimated phase error based on maximum likelihood, °	24.18
Ramachandran plot statistics	
Residues in favored regions, %	94.5
Residues in allowed regions, %	5.5
Residues in disallowed regions, %	0.0

Table S3. Putative $^{8-9}$FnI binding sites on α_1 and α_2 chains of type-I collagen

α_1 chain residues	Sequence
(UniProt-KB/Swiss-Prot: P02452)	
82–90*	GLP GMK GHR
91–99	GFS GLD GAK
94–102	GLD GAK GDA
166–174	GFP GAV GAK
316–324	GFP GAD GVA
355–363	GLP GAK GLT
502–510	GFP GER GVQ
697–705	GFP GAA GRV
775–783	GIA GQR GVV
784–792*	GLP GQR GER
928–936	GIK GHR GFS
α_2 chain residues	
(UniProt-KB/Swiss-Prot: P02452)	
82–90*	GLP GFK GIR
85–93	GFK GIR GHN
88–96	GIR GHN GLD
127–135	GLP GER GRV
214–222	GLT GAK GAA
316–324	GLP GAD GRA
448–456	GVQ GGK GEQ
535–543	GVV GAV GTA
550–558	GLP GER GAA
559–567	GIP GGK GEK
697–705	GFP GAA GRT
784–792*	GLP GSR GER
793–801	GLP GVA GAV
928–936	GLP GLK GHN
931–939	GLK GHN GLQ
940–948	GLP GIA GHH
943–951	GIA GHH GDQ

Asterisks denote predicted high-affinity sites for $^{8-9}$FnI.